# New Empirically Derived Solar Radiation Pressure Model for Global Positioning System Satellites

Y. Bar-Sever[1] and D. Kuang[1]

*We describe the development and testing of a set of new and improved solar radiation pressure models for Global Positioning System (GPS) satellites that is based on four and one-half years of precise GPS orbital data. These empirical models show improved performance in both GPS orbit fit and prediction relative to the state-of-the-art models. Orbit-fit rms is improved 80 percent for Block IIR satellites and 24 percent for Block IIA satellites. Orbit-prediction accuracy improved 58 percent for Block IIR satellites and 32 percent for Block IIA satellites. These new models are designated GSPM.04. It is shown that, after the implementation of these new models, Block IIA and Block IIR satellites perform about the same in orbit fit and in orbit prediction.*

## I. Introduction

Orbiting at an altitude of about 20,000 km, with no drag and with limited sensitivity to the details of the Earth's gravitational pull, the Global Positioning System (GPS) satellites seem in little need of a complex dynamical model. Yet the relatively poor geometry of the observation system (providing mostly radial information), combined with the demand of some applications for extremely high accuracy, creates the need for a very careful modeling of the forces acting on a GPS satellite.

The solar radiation pressure force is the largest perturbation acting on GPS satellites after the gravitational attraction from the Earth, Sun, and Moon, and it is the largest error source in the modeling of GPS orbital dynamics. Various efforts have been made since the inception of the GPS to develop high-fidelity GPS solar radiation pressure models for precise orbit determination. These efforts can be classified under two basic approaches. The ground-model approach is based on pre-launch models and measurements of the spacecraft optical and thermal properties [3,4,6]. The empirical approach uses the observed orbital motion of the spacecraft to infer the solar radiation forces (and other forces) acting on the spacecraft [2,5].[2] This study is a follow up investigation to the work reported by Bar-Sever,[3] using

[1] Tracking Systems and Applications Section.

[2] Y. E. Bar-Sever, *New and Improved Solar Radiation Pressure Models for GPS Satellites Based on Flight Data*, JPL Report (internal document), Jet Propulsion Laboratory, Pasadena, California, 1997.

[3] Ibid.

The research described in this publication was carried out by the Jet Propulsion Laboratory, California Institute of Technology, under a contract with the National Aeronautics and Space Administration.

the same approach to empirically derive a solar radiation pressure model that best explains the observed orbital motion of the GPS spacecraft. We extend Bar-Sever's Fourier expansion to higher degrees and for the first time apply the empirical approach to Block IIR satellites.

Our empirical approach to the derivation of the GPS solar radiation pressure model follows these steps:

(1) Select daily "truth" orbit data from over 4 years of precise daily GPS orbits and form 10-day orbit arcs.

(2) Construct a parameterized model of the solar radiation pressure, generate a nominal trajectory, and estimate the parameters that best fit the trajectory to each of the truth 10-day orbit arcs in a least-squares sense.

(3) Combine the estimates from all satellite arcs into a single set of model parameters for Block IIA and Block IIR satellites, respectively, using a least-squares procedure and utilizing the full covariance information from each 10-day fit.

(4) Evaluate the derived model with orbit data fit and prediction tests.

Using nearly four and one-half years of precise daily GPS orbits (from January 1998 to June 2002), we derived a new solar radiation pressure force model for Block IIR GPS satellites and also improved the empirical solar radiation pressure force model for Block IIA GPS satellites (GSPM.II.97) derived by Bar-Sever.[4] These models show improved ability to fit long arcs of precise GPS orbits, and provide much better orbit-prediction capability. The new models derived here are designated GSPM.IIA.04 (for Block IIA satellites) and GSPM.IIR.04 (for Block IIR satellites).

## II. Selection of Truth Orbits

For our truth orbits, we chose the "final" and most accurate daily GPS orbit solutions that are routinely produced at JPL. With a three-dimensional (3D) error of about 5-cm rms, these orbits are among the most accurate currently available. They are based on the empirical solar pressure model developed by Bar-Sever[5] for the Block II/IIA satellites, and on the Lockheed Martin[6] ground-based solar pressure model for Block IIR satellites. They employ the JPL-developed reduced-dynamics technique to mitigate mismodeling by estimating small time-varying stochastic accelerations [7], as well as a special yaw attitude model [1].

The GPS orbits derived by JPL using ground tracking data are most accurately represented in the Earth-fixed system. However, the dynamic orbit integration is carried out most conveniently in an inertial system. We therefore transform the Earth-fixed truth orbits to the J2000 inertial reference frame using the International Earth Rotation Service (IERS) Final (Bulletin B) Earth Orientation Parameters (EOP). The IERS EOP values are more consistent over time than the JPL-derived EOP values, estimated during the GPS truth orbit generation (see Table 1).

We can now form very long multi-day arcs by concatenating consecutive daily ephemerides. It is clear that the longer the arc the more information about the dynamics can be retrieved from it, and many months of data are needed to resolve the fine details of the solar radiation model. Unfortunately, it is not practical to integrate GPS orbits more than a few days because round-off error will tend to

[4] Ibid.

[5] Ibid.

[6] Lockheed Martin Corporation, *Computer Program Development Specification, Master Control Station, SV Positioning Computer Program, NAVSTAR GPS Operational Control System Segment*, CP-MCSEC-304C, Part 1, Appendix A, May 7, 1993.

**Table 1. Daily orbit overlap rms in the J2000 inertial system using two sets of EOP values to transform Earth-fixed truth orbits to the J2000 inertial frame, in centimeters. Using the IERS EOP values resulted in daily orbit overlap rms in the inertial frame that are essentially the same as the daily overlap rms of orbits in the Earth-fixed system. In subsequent analysis, the IERS EOP parameters were used.**

| Time span | IERS EOP | | | JPL-derived EOP | | |
|---|---|---|---|---|---|---|
| | Radial, cm | Cross track, cm | In track, cm | Radial, cm | Cross track, cm | In track, cm |
| July 1, 1998, to July 7, 1998 | 2.7 | 4.3 | 6.3 | 2.7 | 11.7 | 12.3 |
| July 1, 2002, to July 7, 2002 | 2.1 | 2.3 | 2.8 | 2.1 | 11.3 | 11.5 |

contaminate the integration of the state and variational partials. We found it most practical to perform 10-day integrations; hence, we constructed 10-day-long truth arcs.

To ensure the quality of the truth orbits, we searched through all the daily orbit solutions from January 1, 1998, through July 1, 2002, selecting all the consecutive 10-day arcs for which daily 3D orbit overlap rms was better than 20 cm. We found a total of 2414 arcs, as categorized in Table 2. These orbit data are used in two separate groups, one for Block IIA satellites and the other for Block IIR satellites. Orbit-fitting results in each group are combined into separate sets of solar radiation pressure model parameters. Eclipsing arcs have been removed from this analysis. The modeling of solar radiation pressure during eclipse seasons will be the subject of a follow-up article.

## III. Model Parameterization and Combination of Solutions

Following Fliegel el al. [3], we express the solar radiation model as a truncated Fourier expansion in $\varepsilon$, the Earth–satellite–Sun angle. For GPS satellites following their nominal attitude algorithm, the satellite–Sun geometry is a function only of $\varepsilon$ (see Fig. 1). The forces are expressed in the conventional GPS body-fixed system. For Block II/IIA satellites, the Z-coordinate points from the satellite to the Earth center, the Y-coordinate is in the solar panel beam direction, and the X-coordinate is towards the general Sun direction and completing the right-hand system (see Fig. 2). For Block IIR, the Z-coordinate is defined as for Block II/IIA, but the sense of the X- and Y-coordinates is reversed 180 deg.

Starting from the truncated Fourier expansion of the T20 [3] and T30 [4] models, we experimented with the addition of a few more terms in each coordinate. Terms were added when the fit quality was deemed poor and when the post-fit residuals show the presence of missing harmonics. Terms were removed when they appear to be poorly determined or highly correlated with other terms. After some trial and error, we arrived at the following truncated expansion for the three components of the solar radiation pressure (in $\mathrm{m/s^2}$):

$$F_x = s\,10^{-5}(\mathrm{AU}/r)^2/m(\mathrm{S\_X}_1 \sin\varepsilon + \mathrm{S\_X}_2 \sin 2\varepsilon + \mathrm{S\_X}_3 \sin 3\varepsilon + \mathrm{S\_X}_5 \sin 5\varepsilon + \mathrm{S\_X}_7 \sin 7\varepsilon) \quad (1)$$

$$F_y = \mathrm{C\_Y}_0 + 10^{-5}(\mathrm{AU}/r)^2/m(\mathrm{C\_Y}_1 \cos\varepsilon + \mathrm{C\_Y}_2 \cos 2\varepsilon) \quad (2)$$

$$F_z = s\,10^{-5}(\mathrm{AU}/r)^2/m(\mathrm{C\_Z}_1 \cos\varepsilon + \mathrm{C\_Z}_3 \cos 3\varepsilon + \mathrm{C\_Z}_5 \cos 5\varepsilon) \quad (3)$$

**Table 2. Number of 10-day orbit arcs selected for orbit fit.**

| Quantity | Block IIA | Block IIR |
|---|---|---|
| Number of satellites | 17 | 6 |
| Non-eclipsing arcs | 1723 | 289 |
| Eclipsing arcs | 334 | 68 |

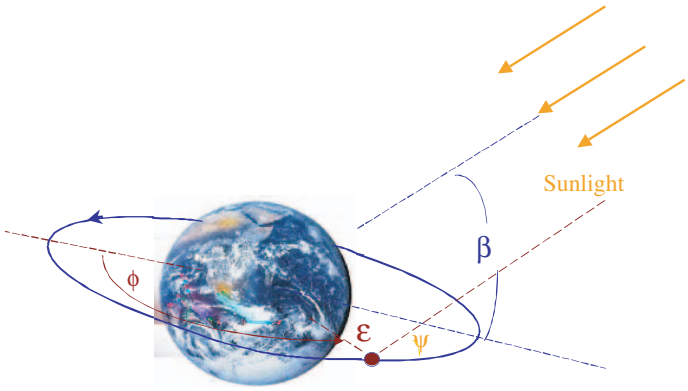


**Fig. 1. The Earth–probe–Sun geometry; β is the angle between the Sun–Earth line and the satellite orbital plane.**

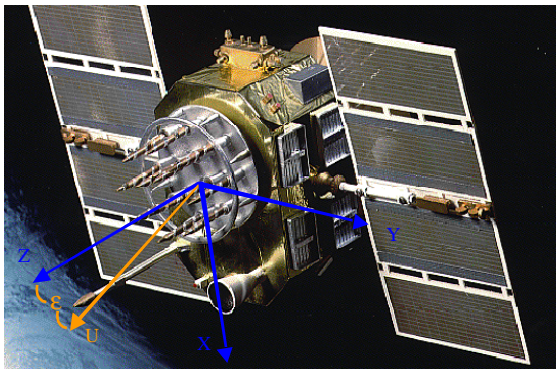


**Fig. 2. GPS satellite attitude and body-fixed system.**

where $s$ is a dimensionless scaling factor, nominally unity; AU is the astronomical unit ($1.4959787066 * 10^8$ km); $r$ is the distance between the spacecraft and the Sun in kilometers; and $m$ is the spacecraft mass in kilograms. The dimension of the Fourier expansion inside the parentheses is, therefore, $10^{-5}$ Newtons ($1\ \mathrm{N} = 1\ \mathrm{kg} * \mathrm{m/s^2}$), enabling easy comparison with the identically dimensioned T20, T30, and GSPM.II.97[7] expansions. (Note, however, that Bar-Sever employs a scale of $\mathrm{nm/s^2}$ in his $F_y$ expansion).

The solar radiation pressure on a satellite is variable due to temporal variations in the solar flux and the spacecraft mass, and to aging effects on the satellite surfaces. These small unmodeled temporal variations are absorbed into the model parameter estimation in each individual satellite arc fit through an overall scale factor. We can think, therefore, of each satellite-arc solution as a slightly scaled realization

[7] Y. E. Bar-Sever, op cit.

of the truth model. To make a robust estimation of the truth model from all the individual samples, we need to combine the estimated parameters across all the arcs while accounting for arc-to-arc variations in scale. To resolve the variable scale, we exploit the fact that S_X$_1$ and C_Z$_1$ are, by far, the dominant components of the radiation force (representing the "push" away from the Sun). We expect, therefore, small variations from arc to arc in the norm of vectors $\langle$S_X$_1$, C_Z$_1\rangle$ with an expected value of 1. For each arc, let $U_0$ be defined as the norm of the vector $\langle$S_X$_1$, C_Z$_1\rangle$. We carry out the combination process in the following steps:

(1) Define $\hat{U}_0$ as the weighted mean of $U_0$ across all satellite-arc solutions.

(2) Scale the X- and Z-components of the parameter vector from each satellite-arc solution by $\hat{U}_0/U_0$.

(3) Find the weighted mean of all the scaled vectors. The result is the combined parameter vector.

This combination process is equivalent to, though simpler than, the combination process in Bar-Sever.[8] When using the combined model within an orbit-determination process, the overall scale factor, $s$ (scaling the X- and Z-components) must be solved for as well as the C_Y$_0$ term (also known as the Y-bias). Note that the Y-components are not scaled.

## IV. Characteristics of the Model Parameters

The individual satellite-arc solutions are divided into two groups for Block IIA and Block IIR. As mentioned above, our empirical solar radiation pressure is assumed to be dependent on a single variable, $\varepsilon$, and otherwise constant in time. We now examine this assumption. If we plot out the estimated force parameters of all 10-day arc solutions as a function of time, we can see that some are in fact not constant. The behavior of these non-constant parameters turns out to be periodic in $\beta$, the angle between the Sun–Earth line and the satellite orbital plane. When this dependency on $\beta$ is strong enough, as is the case for C_Y$_1$ and S_X$_2$ (see Figs. 3 and 4), we prefer to exclude this parameter from the combination across all 10-day arcs, which assumes constancy in time, and instead seek to express that parameter as an explicit function of $\beta$. In the case of C_Y$_1$ and S_X$_2$, we found good fit between the observed variation as a function of $\beta$ and the function

$$F(\beta) = A + B\sin\beta + C/\sin\beta + D\cos\beta \tag{4}$$

We estimated $A$, $B$, $C$, and $D$ in a separate least-squares fit, and the resulting parameters are represented in Tables 3 and 4. This particular dependence of C_Y$_1$ on $\beta$ can be explained as a lag in the yaw attitude of the GPS satellites, which becomes more variable as $\beta$ gets closer to zero. The dependence of the S_X$_2$ parameter on the $\beta$ angle, shown in Fig. 4, needs more investigation. All other model parameters are reasonably constant in time.

## V. Parameter Values and Model Evaluation

### A. The GSPM.04a Model

Following Bar-Sever, the C_Y$_0$ parameter (the Y-bias) is excluded from the combination process. We also exclude from the combination process the parameter C_Y$_1$, which shows significant dependence on the $\beta$ angle, but we ignore the apparent variability of S_X$_2$ and combine it across 10-day arcs as a constant. This simplifies somewhat the model implementation, while having only a minor impact on the quality of

[8] Ibid.

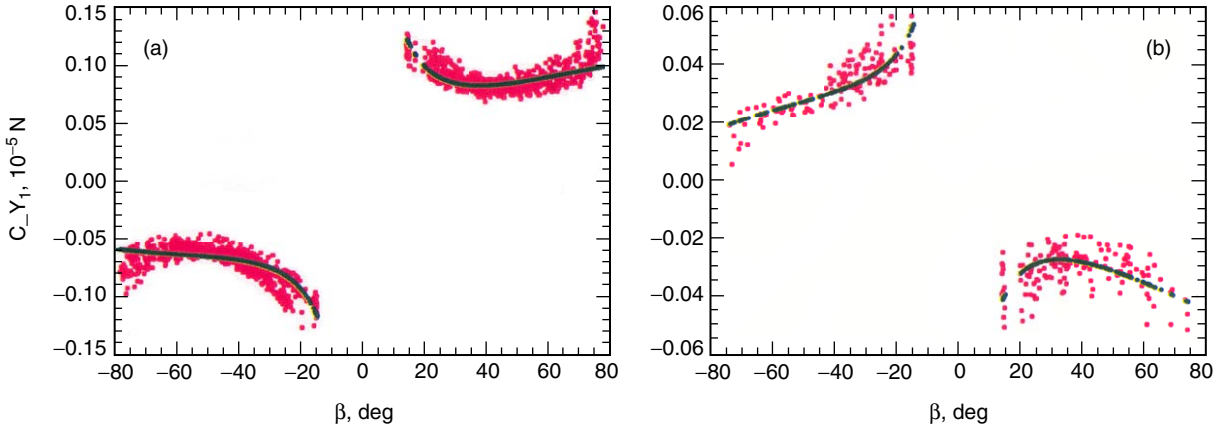


**Fig. 3. Plot of C_$Y_1$ as a function of β (red dots) and the best-fit function $A + B \sin\beta + C/\sin\beta + D\cos\beta$ (green dots) for (a) Block IIA satellites and (b) Block IIR satellites.**

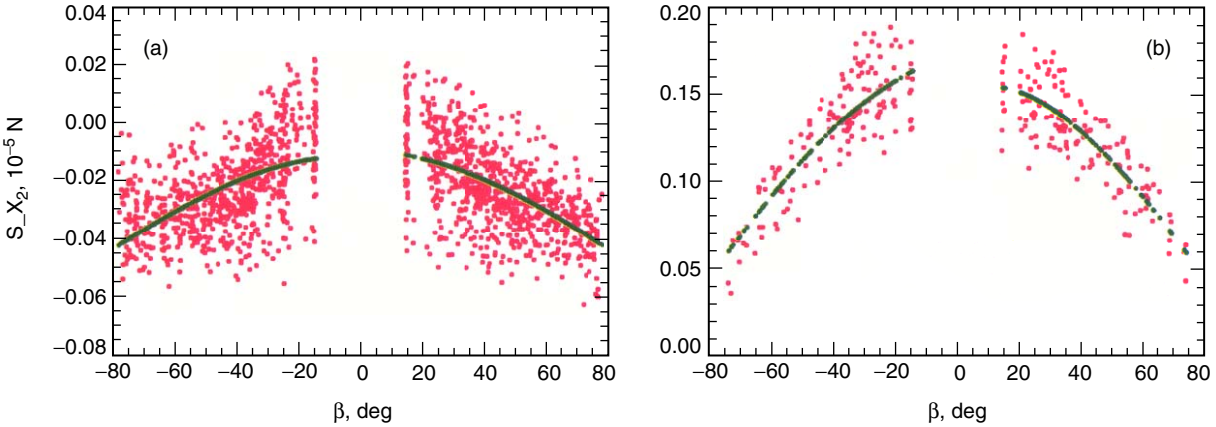


**Fig. 4. Plot of S_$X_2$ as a function of β (red dots) and the best-fit function $A + B \sin\beta + C/\sin\beta + D\cos\beta$ (green dots) for (a) Block IIA satellites and (b) Block IIR satellites.**

the model due to the relatively small magnitude of S_$X_2$. Here, we fit the C_$Y_1$ parameter separately with the ad hoc function of $\beta$, Eq. (4). This model is designated GSPM.04a (for "GPS Solar Pressure Model 2004 Version a"), with the specific designation GSPM.IIA.04a for Block IIA satellites and GSPM.IIR.04a for Block IIR satellites. The values of the combined model parameters are summarized in Table 3. A model that does not assume the constancy of S_$X_2$ (GSPM.04b) is derived in the next subsection.

We evaluated the fidelity of the GSPM.04a model by testing its ability to best fit an independent set of 10-day arcs of truth orbits. In these tests, we fix the model parameters, Eqs. (1) through (3), to the above values and only estimate a solar radiation scale factor, $s$, and a constant Y-bias value for each arc. When the satellite is in Earth eclipse, all the three components are turned off. When $|\beta| < 0.25307$ rad (14.5 deg), we replace the value of $\beta$ in the expression for C_$Y_1$ with 0.25307 if $\beta$ is positive, and with $-0.25307$ if $\beta$ is negative.

Figure 5 illustrates the improvement of the average data fit rms with the new model over the old models (for Block IIA satellites, the nominal model[9] is GSPM.II.97, and for Block IIR it is the Lockheed Martin ground-based model[10]). The improvement in data-fit rms is summarized in Table 4. The rms fit

[9] Ibid.

[10] Lockheed Martin, op cit.

**Table 3. Values of combined solar radiation pressure parameters for the GSPM.04a model, in $10^{-5}$ Newtons.**

| Parameter | Block IIA,[a] $10^{-5}$ N | Block IIR,[a] $10^{-5}$ N |
|---|---|---|
| S_$X_1$ | −8.982 | 10.931 |
| S_$X_2$ | −0.0219 | 0.1279 |
| S_$X_3$ | 0.0151 | 0.2767 |
| S_$X_5$ | 0.1040 | −0.2045 |
| S_$X_7$ | 0.0038 | 0.0568 |
| C_$Z_1$ | −8.6044 | −11.6408 |
| C_$Z_3$ | 0.0158 | 0.0627 |
| C_$Z_5$ | 0.0553 | 0.0674 |
| C_$Y_2$ | 0.01729 | −0.0067 |
| C_$Y_1$[b] | $0.0091 + 0.0539 \sin\beta + 0.0265/\sin\beta$ | $0.0010 - 0.0199 \sin\beta - 0.0107/\sin\beta$ |

[a] Note that Eqs. (1) through (3) are defined with different body-fixed coordinates for Block IIA and Block IIR.

[b] For $|\beta| < 0.25307$ rad (14.5 deg) fix $\beta$ to 0.25307 when $\beta$ is positive and to −0.25307 when $\beta$ is negative.

**Table 4. Performance comparison between the GSPM.04a model and the old solar radiation pressure models, in meters (GSPM.II.97[a] and Lockheed Martin[b] for Block IIA and IIR satellites, respectively).**

| Model | RMS fit to 10-day arcs | | 4th day prediction-error rms | |
|---|---|---|---|---|
| | Block IIA | Block IIR | Block IIA | Block IIR |
| Old model, m | 0.25 | 0.89 | 1.44 | 2.24 |
| GSPM.04a, m | 0.21 | 0.21 | 1.02 | 0.99 |
| Improvement, percent | 16 | 76 | 29 | 56 |

[a] Y. E. Bar-Sever, *New and Improved Solar Radiation Pressure Models for GPS Satellites Based on Flight Data*, JPL Report (internal document), Jet Propulsion Laboratory, Pasadena, California, 1997.

[b] Lockheed Martin Corporation, *Computer Program Development Specification, Master Control Station, SV Positioning Computer Program, NAVSTAR GPS Operational Control System Segment*, CP-MCSEC-304C, Part 1, Appendix A, May 7, 1993.

for Block IIR satellites improves by 76 percent and now is similar to the rms fit of the Block IIA satellites. These show modest improvement (16 percent) over the old model, which was also flight-data driven.

GSPM.04a was also tested for its predictive power. In the prediction test, we fit 4-day arcs of orbit data, and then integrate forward another 4 days using the initial state and force parameters (solar radiation scale factor and Y-bias) estimated from the data fit. The rms of the difference between the predicted orbit and the truth orbit on the final day is computed as the prediction error. The average improvement in prediction error rms is illustrated in Fig. 6 and summarized in Table 4. Again, the improvement for Block IIR satellites is more significant (56 percent) than for Block IIA satellites (29 percent), as expected, bringing the overall orbit predictability of Block IIA and IIR satellites to the same level.

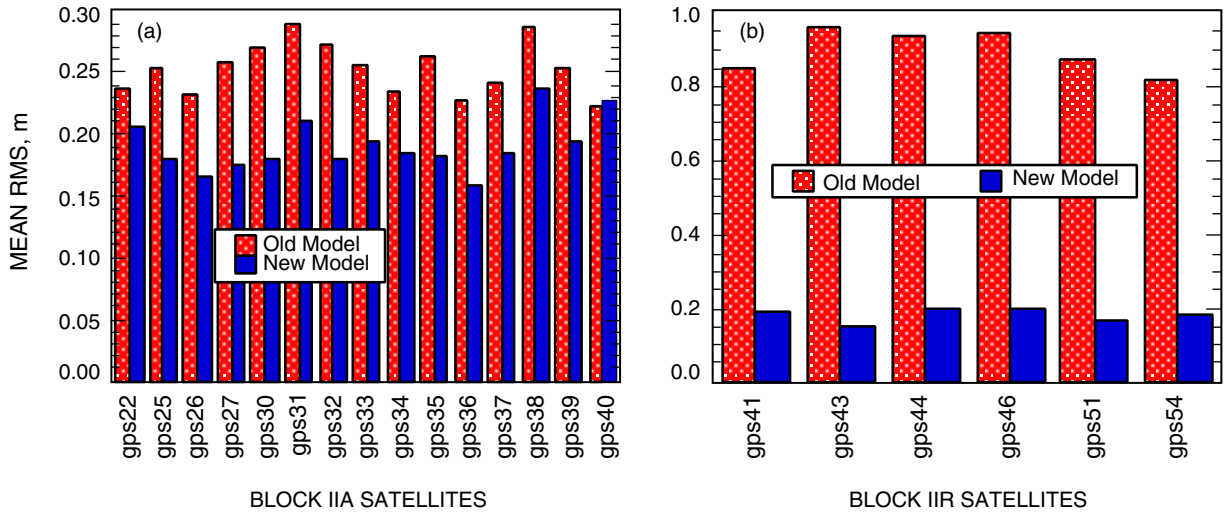


**Fig. 5. Average data-fit rms to 10-day arc truth orbits for (a) Block IIA satellites and (b) Block IIR satellites. The "old" models are Bar-Sever and Lockheed Martin for Block IIA and IIR satellites, respectively. The "new" model is GSPM.04.**

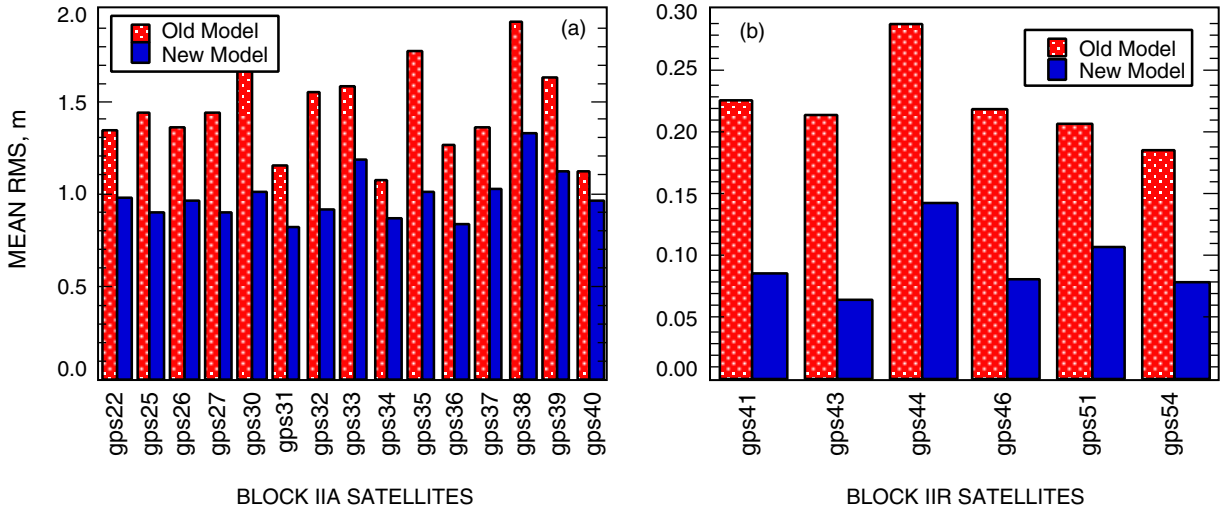


**Fig. 6. Average 4th-day prediction-error rms for (a) Block IIA satellites and (b) Block IIR satellites. The "old" models are Bar-Sever and Lockheed Martin for Block IIA and IIR satellites, respectively. The "new" model is GSPM.04.**

## B. The GSPM.04b Model

We now exclude from the combination process both C_$Y_1$ and S_$X_2$, and fit the C_$Y_1$ and S_$X_2$ parameters separately with the ad hoc function of $\beta$, Eq. (4). The values of the combined model parameters are summarized in Table 5.

The performance of this model in comparison with the old models is summarized in Table 6. It consistently outperforms GSPM.04a (Table 4) by 2 to 8 percentage points. However, we have chosen not to present the analogs of Figs. 3 and 4 because the slight performance edge of GSPM.04b over GSPM.04a will be difficult to discern visually. (In fact, Figs. 3 and 4 actually represent the performance of GSPM.04b).

**Table 5. Values of combined solar radiation pressure parameters for the GSPM.04b model, in $10^{-5}$ Newtons.**

| Parameter | Block IIA,[a] $10^{-5}$ N | Block IIR,[a] $10^{-5}$ N |
|---|---|---|
| S_$X_1$ | $-8.9820$ | 10.9310 |
| S_$X_2$[b] | $-0.0509 + 0.0002\sin\beta$ | $0.0172 + 0.0022\sin\beta$ |
| | $+0.0002/\sin\beta + 0.0407\cos\beta$ | $-0.0016/\sin\beta + 0.1477\cos\beta$ |
| S_$X_3$ | 0.0045 | 0.2476 |
| S_$X_5$ | 0.1060 | $-0.2283$ |
| S_$X_7$ | 0.0028 | $-0.0140$ |
| C_$Z_1$ | $-8.6044$ | $-11.6411$ |
| C_$Z_3$ | 0.0225 | 0.0583 |
| C_$Z_5$ | 0.0543 | 0.0571 |
| C_$Y_2$ | 0.0175 | $-0.0064$ |
| C_$Y_1$[b] | $0.0271 + 0.0459\sin\beta$ | $-0.0195 - 0.0172\sin\beta$ |
| | $+0.0302/\sin\beta - 0.0252\cos\beta$ | $-0.0119/\sin\beta + 0.0272\cos\beta$ |

[a] Note that Eqs. (1) through (3) are defined with different body-fixed coordinates for Block IIA and Block IIR.

[b] For $|\beta| < 0.25307$ rad (14.5 deg) fix $\beta$ to 0.25307 when $\beta$ is positive and to $-0.25307$ when $\beta$ is negative.

**Table 6. Performance comparison between the GSPM.04b model and the old solar radiation pressure models, in meters (GSPM.II.97[a] and Lockheed Martin[b] for Block IIA and IIR satellites, respectively).**

| Model | RMS fit to 10-day arcs | | 4th day prediction-error rms | |
|---|---|---|---|---|
| | Block IIA | Block IIR | Block IIA | Block IIR |
| Old model, m | 0.25 | 0.89 | 1.44 | 2.24 |
| GSPM.04b, m | 0.19 | 0.18 | 0.98 | 0.94 |
| Improvement, percent | 24 | 80 | 32 | 58 |

[a] Y. E. Bar-Sever, *New and Improved Solar Radiation Pressure Models for GPS Satellites Based on Flight Data*, JPL Report (internal document), Jet Propulsion Laboratory, Pasadena, California, 1997.

[b] Lockheed Martin Corporation, *Computer Program Development Specification, Master Control Station, SV Positioning Computer Program, NAVSTAR GPS Operational Control System Segment*, CP-MCSEC-304C, Part 1, Appendix A, May 7, 1993.

## VI. Treatment of Eclipsing Satellites

For the purpose of this analysis, eclipse periods are defined, rather crudely, as spanning $\beta$ angles between $-14.5$ deg and $+14.5$ deg. Eclipsing satellites are much more difficult to model because of their complex attitudes and the intermittent exposure to solar flux [1]. For Block IIA satellites, which exhibit a highly non-linear attitude behavior, we continue to use the GSPM.II.97 model.[11] Block IIR satellites have

[11] Bar-Sever, op cit.

much simpler attitude behavior, and for them we simply extend the above model into the $-14.5$ deg $< \beta$ $< +14.5$ deg regime. However, to avoid the singularity of C_$Y_1$ near $\beta = 0$, we replace $\beta$ with a value of $+14.5$ deg if $\beta$ is positive and with a value of $-14.5$ deg if $\beta$ is negative. During umbra the solar pressure is set to zero, including the Y-bias. During penumbra crossing the full solar pressure model is scaled by the fraction of the Sun disk that is "seen" by the satellite. A future article will analyze the performance of the solar pressure model on eclipsing satellites, utilizing the orbit data spanning $\beta$ angles between $-14.5$ deg and $+14.5$ deg.

## VII. Discussion

Using four and one-half years of precise GPS orbital data, we developed an empirical solar radiation pressure force model using a long arc orbit fit strategy. The new model is a set of Fourier functions of Sun–spacecraft–Earth angle in the GPS satellite body-fixed system. The new models show improved performance in both GPS orbit determination and prediction. Orbit-fit rms is improved by 80 percent for Block IIR satellites and by 24 percent for Block IIA satellites. These new models are designated GSPM.IIA.04 and GSPM.IIR.04 for Block IIA and Block IIR, respectively. Slightly different versions designated "a" and "b" are offered for each block.

The ground-based design process (as opposed to the flight-data-based design process we have used here) is carried out by modeling the spacecraft as a collection of components, each with its own shape, size, and optical and thermal characteristics. Given the nominal mission profile and orbital geometry, the process employs various ray tracing and finite-element and finite-difference techniques to simulate the effects of impinging photons on the spacecraft, and derives the solar radiation model. This is a complicated process because most spacecraft have a complicated shape and are made of many different materials. As a result, it is necessary to make some simplifying assumptions in the simulation. For example, some small sub-structures may be ignored, optical and thermal properties are approximated, and secondary reflections (from one component to the other) may be ignored. The result is usually a fairly good model—if the spacecraft in-orbit behavior does not deviate much from the nominal. But the deficiencies of such an approach are clear:

(1) The in-orbit satellite behavior may deviate from the nominal. Misorientation, bending, and flexing of structures are quite common. For example, the non-nominal Y-bias force can be attributed to solar array misalignment [3] and to a yaw bias.[12] Also, actual aging effects may deviate significantly from the model.

(2) It is impossible to gauge the combined effects of all the approximations, simplifying assumptions, and outright errors that went into the model. Hence, the actual accuracy of the model can only be roughly estimated.

(3) The model is not adjustable or tunable. If accuracy requirements change during the lifetime of the mission, it usually requires a costly redesign process.

A flight-data-based design process, in contrast, has the following advantages:

(1) It reflects actual in-orbit behavior.

(2) It is more accurate, as this study demonstrates. It directly accounts for the combined radiation pressure of all spacecraft components.

[12] Ibid.

(3) It is infinitely tunable and adjustable, i.e., once the design process is set up it can be carried out indefinitely and continuously improve and adjust for spacecraft aging and changing environmental conditions.

(4) It provides a tool for learning about actual in-orbit behavior of satellites and for flagging and monitoring problem satellites.

## Acknowledgments

The authors are grateful to Henry Fliegel for inspiring their work on the GPS solar pressure models and for many valuable technical discussions. The authors also are grateful to Jim O'Toole, Art Dorsey, and Bill Feess for implementing these models and demonstrating their benefits for operational orbit determination in the GPS ground segment. Henry, Jim, Art, and Bill have made numerous helpful suggestions that immensely improved this article, and we thank them for their encouragement and support, as well as their patience.

## References

[1] Y. E. Bar-Sever, "A New Model for GPS Yaw Attitude," *Journal of Geodesy*, vol. 70, pp. 714–723, 1996.

[2] G. Beutler, E. Brockman, W. Gurtner, U. Hugentobler, L. Mervart, M. Rothacher, and A. Verdun, "Extended Orbit Modeling Techniques at the CODE Processing Center of the International GPS Service for Geodynamics (IGS): Theory and Initial Results," *Manusripta Geodaetica*, vol. 19, pp. 367–386, 1994.

[3] H. F. Fliegel, T. E. Gallini, and E. R. Swift, "Global Positioning System Radiation Force Model for Geodetic Applications," *Journal of Geophysical Research*, vol. 97, pp. 559–568, 1992.

[4] H. F. Fliegel and T. E. Gallini, "Solar Force Modeling of Block IIR Global Positioning System Satellites," *Journal of Spacecraft and Rockets*, vol. 33, no. 6, pp. 863–866, 1996.

[5] D. Kuang, H. J. Rim, B. E. Schutz, and P. A. M. Abusali, "Modeling GPS Satellite Attitude Variation for Precise Orbit Determination," *Journal of Geodesy*, vol. 70, pp. 572–580, 1996.

[6] M. Ziebart, P. Cross, and S. Adhya, "Modeling Photon Pressure, the Key to High-Precision GPS Satellite Orbits," *GPS World*, vol. 13, no. 1, pp. 43–50, 2002.

[7] J. F. Zumberge, M. B. Heflin, D. C. Jefferson, M. M. Watkins, and F. H. Webb, "Jet Propulsion Laboratory IGS Analysis Center 1994 Annual Report," in *IGS 1994 Annual Report*, IGS Central Bureau, JPL Publication 95-18, Jet Propulsion Laboratory, Pasadena, California, 1995.